Acta Crystallographica Section D
Biological Crystallography
ISSN 0907-4449

Crystallization and initial X-ray diffraction studies of higher plant photosystem I

Adam Ben-Shem,[a]* Nathan Nelson[a] and Felix Frolow[b]

[a]Department of Biological Chemistry, George S. Wise Faculty of Life Sciences, Tel Aviv University, Israel, and [b]Department of Molecular Microbiology and Biotechnology, George S. Wise Faculty of Life Sciences, Tel Aviv University, Israel

Correspondence e-mail: adam@post.tau.ac.il

Received 18 June 2003
Accepted 21 July 2003

Complete photosystem I from a higher plant (pea; *Pisum sativum*) was isolated, purified and crystallized. The crystals diffract to 4 Å resolution using synchrotron radiation and belong to the monoclinic crystal system, space group $P2_1$, with unit-cell parameters a = 181.90, b = 190.24, c = 219.66 Å, β = 90.484°. Data sets from three crystals have been collected and were merged into a 4.4 Å resolution data set, taking advantage of the high isomorphicity observed for these crystals. Analysis of the self-rotation Patterson function suggests the possible presence of two PSI complexes in the asymmetric unit.

1. Introduction

Photosynthesis converts light energy into biologically useful chemical bonds. The primary energy conversion, where light is applied to initiate an electron-transfer chain, takes place in large membrane complexes termed reaction centres. In plants, two such complexes, photosystem I (PSI) and photosystem II (PSII), operate in concert. Light energy is harnessed by PSII to translocate electrons from water at the inner face of the membrane (lumen) to a quinone moiety at the outer face of the membrane (stroma). Another membrane complex, b_6f, oxidizes the reduced quinones and funnels electrons to a small copper protein, plastocyanin, which in turn binds to PSI. PSI exploits solar energy to transfer electrons from the lumenal plastocyanin through a chain of cofactors to ferredoxin at the outer face of the membrane. The redox potential energy is subsequently 'fixed' in NADPH. The electron transfer from water to $NADP^+$ is coupled to the establishment of a proton gradient across the membrane, which drives the production of ATP by ATP-synthase (Chitnis, 2001). In the dark reaction, ATP and NADPH contribute the chemical energy necessary for the reduction of CO_2 to carbohydrates (Ort & Yocum, 1996).

Higher plant PSI is composed of two moieties: a ~400 kDa core which is the PSI-reaction centre and a peripheral antenna complex, LHCI (Bengis & Nelson, 1975; Mullet *et al.*, 1980; Nelson & Ben-Shem, 2002). The core (PSI-reaction centre) itself comprises 14 subunits denoted PsaA–L, PsaN and PsaO. The PsaA/B hetereodimer forms the heart of PSI and binds the P700 chlorophyll dimer, where light-driven charge separation occurs, as well as being where the first electron acceptors A_0 (chlorophyll *a* molecule), A_1 (phylloquinone) and F_x (4Fe–4S cluster) operate. This heterodimer also coordinates ~90 chlorophylls which serve as an intrinsic light-harvesting antenna. The terminal components of the electron-transfer chain, two additional 4Fe–4S clusters (F_a and F_b), are bound to PsaC. The remaining subunits participate in the docking of ferredoxin (PsaE, PsaD) and plastocyanin (PsaF and PsaN), association of LHCI with the core (PsaK, PsaG and perhaps PsaJ and PsaF as well), binding of LHCII, a light-harvesting complex normally associated with PSII (PsaH and possibly PsaL), maintaining complex integrity and probably other functions (Scheller *et al.*, 2001).

The structure of cyanobacteria PSI, which is homologous to the plant PSI core moiety, was recently solved at 2.5 Å resolution, revealing the position and orientation of all electron-transport components, 96 chlorophylls and 14 carotenoids (Jordan *et al.*, 2001). Four subunits found in the plant PSI core (PsaG, H, N and O) do not have cyanobacterial counterparts.

The peripheral antenna complex LHCI, which is absent in bacterial PSI, is composed of four different transmembrane subunits (Lhca1–Lhca4), which belong to the large super-gene family Lhc (Jansson, 1999). The 20–24 kDa subunits assemble into homodimers or heterodimers which coordinate ~20 chlorophylls (*a* and *b*) as well as several carotenoids (Croce *et al.*, 2002; Schmid *et al.*, 2002). The Lhca proteins are unique among the Lhc family in absorbing light at longer wavelengths (Croce *et al.*, 2002; Ihalainen *et al.*, 2000), however, their general fold would probably be similar to that of LHCII, whose structure was elucidated by electron crystallography (Kuhlbrandt *et al.*, 1994). The exact composition of LHCI is dependant upon light

properties and other environmental factors, but it is thought that under most conditions two copies of each of the four Lhca proteins attach to the PSI core (Jansson *et al.*, 1996).

To advance our understanding of energy migration within and from the peripheral antenna and to gain insight into the evolutionary forces that have shaped the higher plant PSI, we have obtained ordered crystals of the holocomplex (core plus LHCI).

2. Materials and methods

2.1. Thylakoid preparation

Peas (*Pisum sativum* var. Alaska) were grown for 12 d under cool-white fluorescent light (90–130 μE m^{-2} s^{-1}) in a 16 h light/8 h dark cycle. All subsequent steps were carried out at 277 K. Washed leaves (60–75 g) were ground with ice-cold STN buffer (0.3 *M* sucrose, 15 m*M* NaCl, 30 m*M* tricine–NaOH pH 8, 1–2 m*M* PMSF, 15 μ*M* leupeptin, 1 μ*M* pepstatin A) for 15 s. The slurry was filtered through eight layers of cheesecloth and centrifuged for a few seconds. Chloroplasts were then precipitated by centrifugation at 1500*g* for 7 min and suspended in a hypotonic medium (5 m*M* tricine–NaOH pH 8). Starch was removed by a short centrifugation at 500*g* for 2 min. Thylakoids were collected by centrifugation at 20 000*g* for 15 min and resuspended in a buffer containing 5 m*M* tricine–NaOH pH 8 and 150 m*M* NaCl. The last step was repeated twice. Thylakoid membranes were then precipitated and resuspended in minimal volume of STN2 buffer (0.3 *M* sucrose, 20 m*M* tricine–NaOH pH 8, 1 m*M* PMSF). The thylakoid concentration was adjusted to 2.6 mg of chlorophyll per millilitre and the detergent dodecyl maltoside (Anatrace) was added to a final concentration of 0.55%(*w*/*v*) (2.3 mg detergent per milligram of chlorophyll), which was found to selectively extract ATP-synthase, b_6f complex and PSII. After 12 min incubation, detergent-treated thylakoid membranes were collected by ultracentrifugation at 150 000*g* for 30 min, the pellet was resuspended in a minimal volume of STN2 buffer and stored at 193 K unless used immediately. Absorbance at 663 and 645 nm was used to measure chlorophyll concentration after extraction by 80% acetone (Arnon, 1949).

2.2. PSI purification

Thylakoids (10.5–11.5 mg of chlorophyll per purification batch) were solubilized using dodecyl maltoside (DM) at 6.0–6.5 mg detergent per milligram of chlorophyll. Unsolubilized material was removed by ultracentrifugation at 150 000*g* for 13 min. The supernatant was applied to a DEAE-cellulose column (10 cm length, 1.5 cm internal diameter) which had been pre-equilibrated with 10 m*M* Tris–HCl pH 7.4. PSI was eluted after a short wash step (22.5 ml 20 m*M* tricine–Tris pH 7.4, 0.2% DM) with 0–400 m*M* NaCl gradient in buffer containing 20 m*M* tricine–Tris pH 7.4, 0.15% DM (flow rate = 0.8 ml min^{-1}). The first dark green fractions contained mainly PSI including the light-harvesting proteins. PEG 6000 was added to PSI-containing fractions until turbidity appeared. Aggregated proteins were precipitated by centrifugation at 17 000*g* for 10 min, resuspended in Tricine buffer and applied to a 6–40% sucrose gradient in tricine buffer that contained 0.05% dodecyl thiomaltoside (DTM) instead of DM. Following ultracentrifugation (37 000 rev min^{-1}, 16.5 h, Beckman SW40 rotor), monomeric PSI appeared as a wide dark band. Only the middle section of this band could be used further in order to avoid contamination from other thylakoid complexes and aggregated or impaired PSI. Fractions containing monomeric PSI were loaded on a small DEAE-cellulose column (5 cm length, 0.5 cm internal diameter) pre-equilibrated with 20 m*M* tricine–Tris pH 7.3 and 0.01% DTM. After a short wash step (8–10 ml 20 m*M* tricine–Tris pH 7.3, 40–50 m*M* ammonium acetate, 0.045% DTM), PSI was eluted by a solution containing 20 m*M* tricine–Tris pH 7.3, 200–220 m*M* ammonium acetate and 0.045% DTM. Purified PSI was immediately precipitated by PEG 6000, resuspended and used for crystallization. The complex was shown to be active in P700 light-induced oxidation by measurements of reduced minus oxidized spectra using a dual-wavelength spectrometer at 430–540 nm according to Hiyama & Ke (1972).

The detergent-to-chlorophyll ratio had to be carefully optimized in all steps and proved to be a crucial factor for producing ordered crystals. It had to be readjusted following changes in pea seed batch, age or growing conditions.

2.3. Crystallization

Crystallization trials were set up using the sitting-drop variant of the vapour-diffusion technique at 277 K. 4 µl drops of purified protein at 2 mg chlorophyll per millilitre (~7 mg ml^{-1} protein) were mixed with equal volumes of reservoir solution [22.5 m*M* MES–bis-tris pH 6.6, 0.5%(*v*/*v*) PEG 400, 8.1 m*M* ammonium citrate, 5.6–6.4%(*w*/*v*) PEG 6000] and equilibrated against 0.5 ml reservoir solution. Crystals appeared within 2–3 d and reached maximum size within two weeks. Their quality was severely impaired after an additional two weeks (loss of sharp edges, degradation of diffraction quality). As with several other large complexes, the formation of crystals within a relatively short time seems to be essential in order to retain the complex integrity (*e.g.* Yonath *et al.*, 1982; Zhang *et al.*, 2003). Typical crystallization results are shown in Fig. 1(*a*). The presence of PSI in the crystals was confirmed by SDS–PAGE on a crystal carefully washed using reservoir solution. The upper bands in the resulting gel (Fig. 1*b*) correspond to subunits *A*, *B* and Lhca1-4, whilst the lower band corresponds to the smaller subunits, which are not separated in this gel.

2.4. In-house crystal characterization and crystal selection

Our in-house X-ray facilities, comprising a Rigaku Ultrax 18X direct-drive rotating-anode generator operating at 50 kV and 100 mA, OSMIC multilayer confocal mirrors and a Rigaku R-AXIS IV imaging-plate area detector, were not suitable for

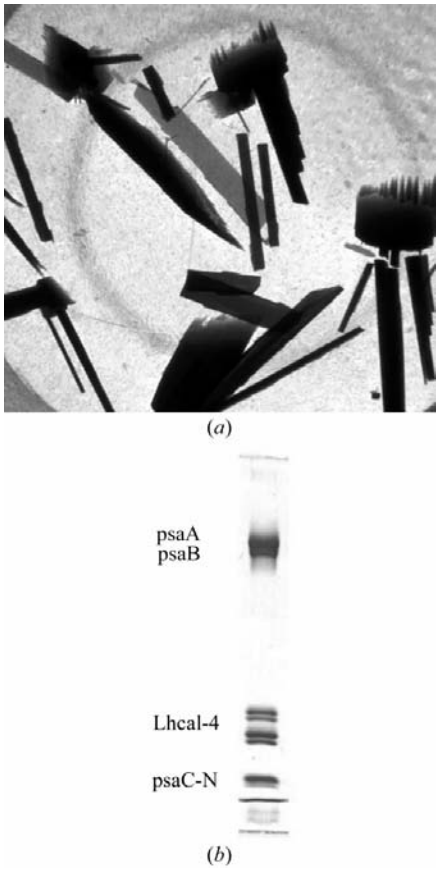

Figure 1
(*a*) Crystals of pea PSI; (*b*) SDS–PAGE gel of a washed crystal.

efficient data collection from the crystals of PSI. However, they were used successfully for crystal characterization, tuning of the crystallization procedure and for the selection of crystals for synchrotron data-collection measurements.

Crystals obtained in the first crystallization experiments diffracted to about 20 Å in-house. The diffraction resolution limit of the crystals was gradually extended to 6 Å by optimization of the preparation, crystallization and cryoconditions. As is frequently observed for membrane proteins, small alterations in the purification method (*e.g.* in the detergent-to-chlorophyll ratio) resulted in a significant improvement in crystal quality. Optimizing the pea type and growing conditions and adjusting the preparation to seasonal changes were essential.

Prior to data collection, crystals were transferred in two steps to a cryosolution (22.5 m*M* MOPS–bis-tris pH 6.8, 21.5 m*M* ammonium tartrate, 0.5% PEG 400, 25% ethylene glycol and 15% PEG 6000) and left to equilibrate for 5–6 h. The higher PEG 6000 concentration in the cryosolution proved necessary to render rigidity on the crystals.

Crystals were mounted in a cryoloop (Teng, 1990), cooled directly in a 100 K nitrogen-gas stream (Oxford Cryosystems; Cosier & Glazer, 1986), tested for diffraction quality and stored in a liquid-nitrogen dewar for later use at the synchrotron source.

2.5. Correlation between in-house and synchrotron diffraction power

To optimize crystal selection for the transport of frozen crystals to the synchrotron facility, all crystals were checked for diffraction limit using in-house equipment and only crystals with the best diffraction were chosen. For the first visit to a synchrotron, several crystals were carefully selected to represent several resolution limits ranging between 9 and 7 Å in order to correlate diffraction limits between in-house and synchrotron sources. Diffraction experiments performed at ESRF with these crystals showed that the resolution limits were not extended in a linear manner. For crystals diffracting in-house to approximately 7 Å, the diffraction limit at ESRF was extended to 4 Å; the diffraction limit was extended to a significantly lesser extent for crystals with lower in-house resolution. This in-house selection appeared to be highly effective, as only one of several crystals diffracted to 7 Å and approximately only one in every four protein preparations produced such crystals.

Table 1
X-ray data-collection statistics of PSI crystals.

Values in parentheses are for the last resolution bin (4.52–4.44 Å).

	Crystal 1	Crystal 2	Crystal 3	Merged data
X-ray source	ID14-1, ESRF	ID14-4, ESRF	ID14-1, ESRF	
Wavelength (Å)	0.933	0.9393	0.933	
Space group	$P2_1$	$P2_1$	$P2_1$	$P2_1$
Unit-cell parameters				
a (Å)	182.3	181.8	181.4	181.9
b (Å)	190.4	190.2	189.9	190.2
c (Å)	220.2	219.7	218.9	219.66
β (°)	90.5	90.4	90.4	90.4
Mosaicity (°)	0.87	0.71	1.11	
No. of observations	301035	275512	308093	862552
Unique reflections	88145	90029	93002	92318
Data completeness (%)	95.1 (87.5)	96.6 (96.8)	98.0 (93.5)	99.6 (99.5)
$\langle I/\sigma(I)\rangle$	12.6 (1.2)	13.9 (1.5)	12.5 (1.2)	18.8 (2.0)
$R_{\rm sym}$† (%)	0.073 (0.86)	0.078 (0.59)	0.079 (0.82)	0.099 (0.86)

† $R_{\rm sym} = \sum |I - \langle I\rangle| / \sum I$.

2.6. Synchrotron data collection

Crystals were tested on either beamline ID14-1 or ID14-4 at ESRF, Grenoble with a fixed wavelength of 0.930 Å. Three data sets were collected from crystals which diffracted to a 4.0 Å resolution limit (Fig. 2). Typical orientation of the elongated plate-like crystals in the cryoloops was with the large face in the plane of the loop and the long crystal dimension along the loop. However, an attempt was made to use various orientations during crystal mounting. Data were collected at a distance of 400 mm from the crystal, with each frame being 0.5° in width, using an exposure of 5 or 10 s (ID14-4) or 30 s (ID14-1) per frame for a total rotation of 180°. During data collection crystals were translated two or three times along the rotation axis. Owing to radiation damage, data were integrated and scaled to a maximum resolution of 4.44 Å for each individual crystal using the *HKL* suite (Otwinowski & Minor, 1997). The final data set was created by merging all three crystals using *SCALEPACK* (part of the *HKL* suite) and was converted to structure factors using *TRUNCATE* (Collaborative Computational Project, Number 4, 1994). A summary of the X-ray data-collection statistics can be found in Table 1.

2.7. Self-rotation function

A self-rotation function was calculated using *POLARRFN* (Kabsch, unpublished work; Collaborative Computational Project, Number 4, 1994) and exhibits a peak (3σ, the highest peak after peaks generated by the crystallographic twofold) on $\kappa = 180°$ with $\varphi = 180°$ and $\omega = 166°$ (Fig. 3). The nature of this non-crystallographic symmetry is not yet clear. It may reflect the presence of non-

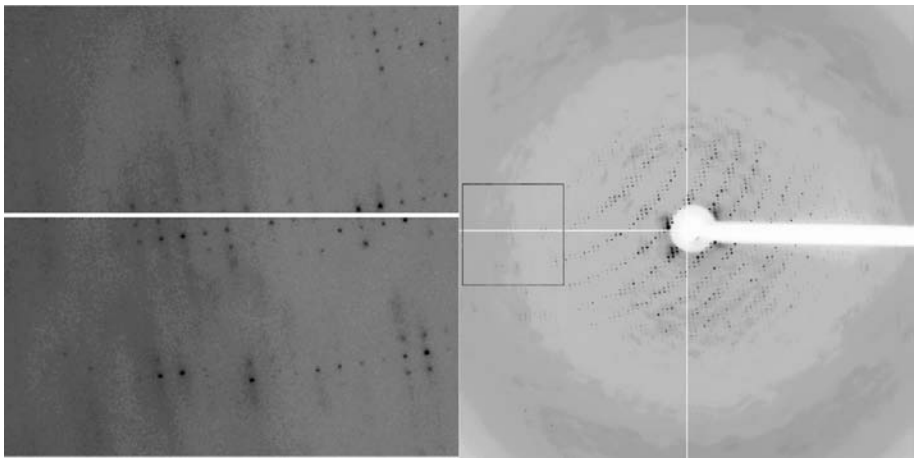

Figure 2
A 0.5° rotation diffraction pattern from a PSI crystal collected at ESRF ID14-4 using an ADSC CCD area detector. The resolution at the edge of the pictures is 4.0 Å.

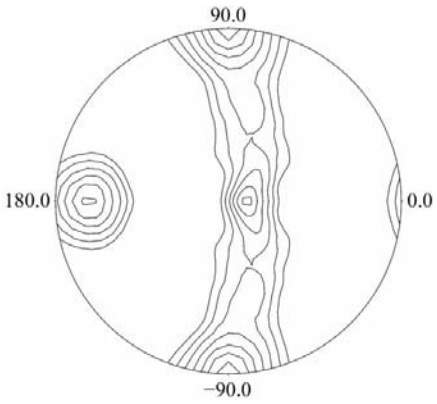

Figure 3
κ = 180° section of the self-rotation function calculated from the native data set of a PSI crystal. The resolution of the data used was 50–4.5 Å. The highest non-crystallographic peak at φ = 180° and ω = 166° corresponds to the direction of the non-crystallographic twofold axis; its height is 90% of the origin.

crystallographic symmetry between two independent molecules in the unit cell or of non-crystallographic symmetry between two pseudo-symmetric parts of the PSI molecule, similar to that observed for PSI from cyanobacteria (Schubert *et al.*, 1997). The Matthews coefficients (Matthews, 1968) calculated for three, two and one molecules in the asymmetric unit (assuming an approximate molecular weight of 600 kDa) were 2.1 (41.6% solvent), 3.2 (61.1% solvent) and 6.4 Å^3 Da^{-1} (80.5% solvent), respectively, suggesting the presence of the two PSI complexes in the asymmetric unit. Notwithstanding the Matthews coefficient, the presence of a trimer in the asymmetric unit is unlikely owing to the observation that for most membrane proteins the solvent content is much higher than that of water-soluble proteins (*e.g.* a solvent content of 80% in cyanobacterial PSI; Schubert *et al.*, 1997).

3. Results and discussion

Crystals of pea PSI measured 0.6 × 0.3 × 0.1 mm (Fig. 1*a*) and diffracted to approximately 4.0 Å resolution (Fig. 2). The crystals belong to the monoclinic crystal system, space group $P2_1$, with unit-cell parameters a = 181.90, b = 190.24, c = 219.66 Å, β = 90.484° and a mosaicity of about 0.7–1.1°. The angle β is relatively close to 90° and a decision about the selection of a consistent orientation of the crystals (practically converted to a systematic selection between a β angle larger or smaller than 90°) was made during the merging procedure and, if necessary, a transformation was applied. In addition, the possibility of a higher orthorhombic space group was ruled out on the basis of the results of merging symmetry-related reflections: the average R factor for space group $P2_1$ is about 8%, while the respective R factor for space group $P222$ is about 56%.

The decision to include higher resolution data in the data sets was made on the basis of the signal-to-error ratio in the corresponding resolution shells rather than on the basis of the $R_{\rm sym}$ factor. The decision to include higher resolution shells in the combined data set was made on the basis of the improvement of the signal-to-error ratio relative to the individual data (see Table 1) and revealed 4.44 Å resolution. If a conservative approach (based on an R factor of about 45%) is used, the resolution is about 4.60 Å.

The three crystals used to construct the complete data set have been obtained from different preparations, yet the diffraction data collected from them did not suffer from lack of isomorphism. This observation might have important consequences during future work with heavy-atom derivative crystals.

A search for heavy-atom derivatives and attempts to solve the structure using molecular replacement with the bacterial PSI system as a model are currently in progress.

PSI appears as a trimer in cyanobacteria (Jordan *et al.*, 2001). The migration of the complex from pea thylakoids in the sucrose gradient indicates that the complex from higher plants is purified as a monomer. Therefore, since there is no evidence for dimeric or trimeric PSI in plant thylakoid membranes, we believe that if there are indeed two complexes in the asymmetric unit, they do not form a membranal dimer. The potential presence of two molecules in the asymmetric unit will be exploited during density-modification procedures using NCS averaging.

We thankfully acknowledge the ESRF for synchrotron beam time and the staff scientists of the ID14 station cluster for their assistance. AB acknowledges the Charles Clore Foundation for a PhD student scholarship and is grateful to Dr N. Ohad and Professor Y. Anikster for providing access to plant-growing facilities and to Hannan Bushary for sharing expertise in pea growing. This work was supported by the Israel Science Foundation grant (No. 403/02 to NN and FF). We acknowledge support by Tel Aviv University Institute of Structural Biology (TAU-ISB). AB dedicates his share of the work described here to the memory of his friend Joe, who passed away during the preparation of this article.

References

Arnon, D. I. (1949). *Plant Physiol.* **2**, 1–15.
Bengis, C. & Nelson, N. (1975). *J. Biol. Chem.* **250**, 2783–2788.
Chitnis, P. R. (2001). *Annu. Rev. Plant Physiol. Plant Mol. Biol.* **52**, 593–626.
Collaborative Computational Project, Number 4 (1994). *Acta Cryst.* D**50**, 760–763.
Cosier, J. & Glazer, A. M. (1986). *J. Appl. Cryst.* **19**, 105–107.
Croce, R., Morosinotto, T., Castelletti, S., Breton, J. & Bassi, R. (2002). *Biochim. Biophys. Acta*, **1556**, 29–40.
Hiyama, T. & Ke, B. (1972). *Biochim. Biophys. Acta*, **267**, 160–171.
Ihalainen, J. A., Gobets, B., Sznee, K., Brazzoli, M., Croce, R., Bassi, R., van Grondelle, R., Korppi-Tommola, J. E. I. & Dekker, J. P. (2000). *Biochemistry*, **39**, 8625–8631.
Jansson, S. (1999). *Trends Plant Sci.* **4**, 236–240.
Jansson, S., Andersen, B. & Scheller, H. V. (1996). *Plant Physiol.* **112**, 409–420.
Jordan, P., Fromme, P., Witt, H. T., Klukas, O., Saenger, W. & Krauss, N. (2001). *Nature (London)*, **411**, 909–917.
Kuhlbrandt, W., Wang, D. N. & Fujiyoshi, Y. (1994). *Nature (London)*, **367**, 614–621.
Matthews, B. W. (1968). *J. Mol. Biol.* **33**, 491–497.
Mullet, J. E., Burke, J. J. & Arntzen, C. J. (1980). *Plant Physiol.* **65**, 814–822.
Nelson, N. & Ben-Shem, A. (2002). *Photosynth. Res.* **73**, 193–206.
Ort, D. R. & Yocum, C. F. (1996). *Oxygenic Photosynthesis: The Light Reaction*, edited by D. R. Ort & C. F. Yocum, pp. 1–9. Dordrecht: Kluwer Academic Publishers.
Otwinowski, Z. & Minor, W. (1997). *Methods Enzymol.* **276**, 307–326.
Scheller, H. V., Jensen, P. E., Haldrup, A., Lunde, C. & Knoetzel, J. (2001). *Biochim. Biophys. Acta*, **1507**, 41–60.
Schmid, V. H. R., Potthast, S., Wiener, M., Bergauer, V., Paulsen, H. & Storf, S. (2002). *J. Biol. Chem.* **277**, 37307–37314.
Schubert, W. D., Klukas, O., Krauss, N., Saenger, W., Fromme, P. & Witt, H. T. (1997). *J. Mol. Biol.* **272**, 741–769.
Teng, T.-Y. (1990). *J. Appl. Cryst.* **23**, 387–391.
Yonath, A., Mussig, J. & Wittmann, H. G. (1982). *J. Cell. Biochem.* **19**, 145–155.
Zhang, H. M., Kurisu, G., Smith, J. L. & Cramer, W. A. (2003). *Proc. Natl Acad. Sci. USA*, **100**, 5160–5163.